Feruloyl-CoA 6′-Hydroxylase1-Dependent Coumarins Mediate Iron Acquisition from Alkaline Substrates in Arabidopsis[1][C][W][OPEN]

Nicole B. Schmid, Ricardo F.H. Giehl, Stefanie Döll, Hans-Peter Mock, Nadine Strehmel, Dierk Scheel, Xiaole Kong, Robert C. Hider, and Nicolaus von Wirén*

Department of Physiology and Cell Biology, Leibniz Institute for Plant Genetics and Crop Plant Research, Corrensstrasse 3, 06466 Gatersleben, Germany (N.B.S., R.F.H.G., S.D., H.-P.M., N.v.W.); Department of Stress and Environmental Biology, Leibniz Institute for Plant Biochemistry, Weinberg 3, 06120 Halle, Germany (N.S., D.S.); and Division of Pharmaceutical Science, King's College, 150 Stamford Street, London SE1 9NH, United Kingdom (X.K., R.C.H.)

ORCID IDs: 0000-0002-8836-0419 (N.B.S.); 0000-0003-1006-3163 (R.F.H.G.); 0000-0002-0001-8302 (S.D.); 0000-0002-4966-425x (N.v.W.).

Although iron (Fe) is one of the most abundant elements in the earth's crust, its low solubility in soils restricts Fe uptake by plants. Most plant species acquire Fe by acidifying the rhizosphere and reducing ferric to ferrous Fe prior to membrane transport. However, it is unclear how these plants access Fe in the rhizosphere and cope with high soil pH. In a mutant screening, we identified 2-oxoglutarate-dependent dioxygenase Feruloyl-CoA 6′-Hydroxylase1 (F6′H1) to be essential for tolerance of Arabidopsis (*Arabidopsis thaliana*) to high pH-induced Fe deficiency. Under Fe deficiency, F6′H1 is required for the biosynthesis of fluorescent coumarins that are released into the rhizosphere, some of which possess Fe(III)-mobilizing capacity and prevent *f6′h1* mutant plants from Fe deficiency-induced chlorosis. Scopoletin was the most prominent coumarin found in Fe-deficient root exudates but failed to mobilize Fe(III), while esculetin, i.e. 6,7-dihydroxycoumarin, occurred in lower amounts but was effective in Fe(III) mobilization. Our results indicate that Fe-deficient Arabidopsis plants release Fe(III)-chelating coumarins as part of the strategy I-type Fe acquisition machinery.

Iron (Fe) is an essential element for virtually all forms of life and often limits growth and reproduction (Beinert et al., 1997; Massé and Arguin, 2005). Despite its high abundance in soils, Fe precipitates with phosphates or hydroxyl ions in well-aerated soils already at slightly acidic to alkaline pH levels (Lemanceau et al., 2009; Marschner, 2012). These reactions make Fe sparingly soluble for microorganisms and plants, which are ultimately responsible for entering Fe into the food chain.

To overcome the problem of low Fe solubility, plants have evolved a set of mechanisms to acquire and take up this micronutrient from the soil. All nongraminaceous plants employ a reduction-based strategy (strategy I) to acquire Fe (Kim and Guerinot, 2007; Kobayashi and Nishizawa, 2012). This mechanism includes an enhanced release of protons into the rhizosphere, a process that is mainly related to Fe deficiency-induced proton-translocating adenosine triphosphatases, such as *AHA2* in Arabidopsis (*Arabidopsis thaliana*; Santi and Schmidt, 2009). Released protons decrease the pH of the rhizosphere and thereby facilitate the dissolution of Fe(III) precipitates. Ferric Fe is then reduced to ferrous Fe by the plasma membrane-bound FERRIC CHELATE REDUCTASE2 (FRO2; Robinson et al., 1999; Connolly et al., 2003). This reduction step is a prerequisite for the subsequent transport of Fe^{2+} across the plasma membrane via the IRON-REGULATED TRANSPORTER1 (IRT1; Eide et al., 1996; Varotto et al., 2002; Vert et al., 2002). At the transcriptional level, the individual components of the strategy I are regulated by the cooperative action of the basic helix-loop-helix (bHLH) transcription factors FER-LIKE IRON DEFICIENCY-INDUCED TRANSCRIPTION FACTOR (FIT) and bHLH38 and bHLH39 (Colangelo and Guerinot, 2004; Jakoby et al., 2004; Yuan et al., 2008). This highly coordinated transcriptional regulation of the Fe acquisition machinery allows plants enhancing Fe intake when Fe is limited or when the plant's demand for Fe has increased (Giehl et al., 2009).

Reduction-based Fe acquisition, however, is suppressed by high pH and the presence of bicarbonates. In fact, in calcareous soils, the protons released by Fe-deficient plants are buffered by bicarbonate (Ohwaki and Sugahara, 1997) and the activity of the ferric chelate reductase can be largely repressed (Romera et al., 1997; Alcantara

[1] This work was supported by the Bundesministerium für Bildung und Forschung, Germany (FKZ 0315458B) and the Leibniz Association Germany.

* Address correspondence to vonwiren@ipk-gatersleben.de.

The author responsible for distribution of materials integral to the findings presented in this article in accordance with the policy described in the Instructions for Authors (www.plantphysiol.org) is: Nicolaus von Wirén (vonwiren@ipk-gatersleben.de).

[C] Some figures in this article are displayed in color online but in black and white in the print edition.

[W] The online version of this article contains Web-only data.

[OPEN] Articles can be viewed online without a subscription.

www.plantphysiol.org/cgi/doi/10.1104/pp.113.228544

et al., 2000; Lucena et al., 2007). Under these conditions, the reduction-based mechanism can stall. By contrast, most graminaceous plants perform better in calcareous or alkaline soils, because their Fe acquisition strategy relies on the release of mugineic acid-type, hexadentate chelators, so-called phytosiderophores (Takagi et al., 1984; Nozoye et al., 2011). These organic compounds form complexes with ferric Fe and are then taken up as an intact Fe(III)-phytosiderophore complex without the requirement of a reduction step (Curie et al., 2001; Schaaf et al., 2004). Unlike reduction-based Fe acquisition, phytosiderophore-dependent Fe chelation and uptake is largely insensitive to high soil pH (Römheld and Marschner, 1986).

As approximately one-third of the world's soils are calcareous (Chen and Barak, 1982), many crop species with reduction-based Fe acquisition, such as soybean (*Glycine max*) or potato (*Solanum tuberosum*), are often cultivated on calcareous soils. Although calcareous growth conditions generally reduce the productivity of strategy I plants, there are large differences among strategy I species and genotypes in their tolerance to Fe deficiency-induced chlorosis. To a certain extent, these differences may relate to sequence deviations in FIT- and bHLH-type transcription factors that are primarily thought to drive IRT1- and FRO2-dependent Fe uptake (Peiffer et al., 2012). However, to date, it still remains unknown how nongraminaceous plants access ferric Fe in the rhizosphere and overcome the problem of low Fe solubility and impeded Fe reducibility in high pH soils. One assumption is that strategy I plants induce additional mechanisms to assist and/or complement the reduction-based Fe acquisition machinery. In this regard, it has been shown that Fe deficiency also stimulates the exudation of organic compounds, such as phenolics, organic acids, sugars, and flavins (Römheld and Marschner, 1983; Welkie, 2000; Jin et al., 2007; Carvalhais et al., 2011; Rodríguez-Celma et al., 2011). These compounds could help plants to mobilize sparingly available Fe from the rhizosphere soil or from the root apoplast. For instance, when phenolic compounds released by roots of red clover (*Trifolium pratense*) were removed from the nutrient solution by a synthetic adsorbent, plants developed symptoms of Fe deficiency (Jin et al., 2007). Such an effect was found to be associated with an increased accumulation of Fe in the root apoplast of Fe-deficient plants, indicating that these compounds play a role in the solubilization and utilization of apoplastic Fe. Likewise, the reutilization of Fe that is precipitated in the stele of rice (*Oryza sativa*) roots involves the efflux of the phenols protocatechuic acid and caffeic acid via the MULTIDRUG AND TOXIN EXTRUSION transporter PHENOLICS EFFLUX ZERO1 (Ishimaru et al., 2011b). Alternatively, root exudates may stimulate the microbial activity in the rhizosphere, allowing plants to indirectly profit from microbial dissolution of soil Fe.

Recently, two reports have shown that Fe-deficient Arabidopsis plants produce and release fluorescent phenolic compounds into the growth media (Fourcroy et al., 2013; Rodríguez-Celma et al., 2013). Although in both cases it was shown that these compounds are important to prevent the development of leaf chlorosis, neither study explored how these compounds improved the plants' ability to cope with limited Fe availability. In vitro studies have shown that phenolic compounds can chelate and reduce Fe(III) (Andjelkovic et al., 2006; Mladenka et al., 2010). However, it is noteworthy that the overall reducing capacity of the phenolics released by Fe-deficient roots is many orders of magnitude below that of the ferric chelate reductase (Römheld and Marschner, 1983). Thus, the chemical action and precise nutritional function of the phenolic compounds released by Fe-deficient plants still remains unknown. In addition, it is not yet clear whether and how these compounds help plants to access Fe under calcareous conditions.

To identify genes involved in Fe acquisition under alkaline soil conditions, we simulated an intact rhizosphere and screened transfer DNA (T-DNA) insertion mutants of Arabidopsis on a peat-based substrate supplemented with bicarbonate. One insertion line showing severe symptoms of Fe deficiency turned out to carry a deletion in a gene involved in the phenylpropanoid pathway. Further genetic and biochemical analyses of this mutant provided evidence that Fe deficiency enhances the release of coumarins, which appear to play a crucial role in Fe acquisition under alkaline soil conditions. We show here that these root exudates are directly mediating Fe mobilization, suggesting that also strategy I plants employ chelator-based Fe acquisition strategies.

RESULTS

Isolation of a T-DNA Insertion Line with Strong Chlorosis under Calcareous Conditions

We reasoned that forward genetic approaches directed to identify new components involved in Fe acquisition require the simulation of an intact, high pH rhizosphere. To pursue this aim, we screened a collection of 3,500 homozygous, nonredundant T-DNA insertion lines from Arabidopsis (Alonso et al., 2003) on a peat-based substrate supplemented with calcium carbonate and bicarbonate to yield a pH of 7.2 causing low Fe availability. When compared with nonalkaline conditions (pH 5.6), pH buffering led to growth depression and slight chlorosis in wild-type plants (Fig. 1, A and B). Interestingly, we identified one insertion line (SALK_132418C) that exhibited even stronger chlorosis in its youngest leaves than the wild type as a consequence of significantly lower chlorophyll and Fe concentrations in the shoot (Fig. 1, A–C). Shoot fresh weight was reduced under alkaline conditions, but not significantly different in mutant and wild-type plants after the supply of Fe(III)-EDDHA [for ethylendiamine di(*o*-hydroxyphenylacetic) acid] or when plants were grown at pH 5.6 (data not shown). Because leaf chlorosis

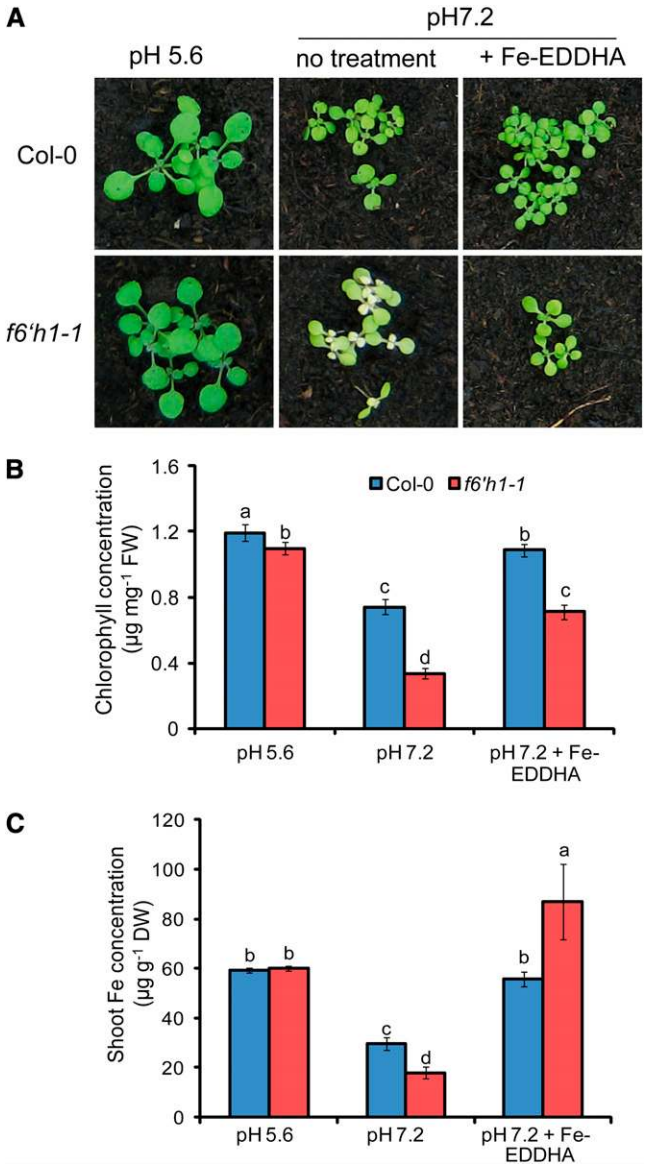

Figure 1. Phenotypic characterization of *f6′h1-1*, a T-DNA insertion line defective in the expression of the 2-oxoglutarate-dependent dioxygenase F6′H1. A, Wild-type (Col-0) and *f6′h1-1* mutant plants were grown for 17 d on nonlimed substrate at pH 5.6 or limed substrate at pH 7.2. To alleviate leaf chlorosis at pH 7.2, plants were supplied with Fe(III)-EDDHA. Chlorophyll (B) and Fe (C) concentrations in shoots of wild-type and *f6′h1-1* plants grown as indicated in A. Bars represent means ± SE (n = three to nine biological replicates). Different letters indicate significant differences according to Tukey's test ($P < 0.05$). FW, Fresh weight; DW, dry weight.

was absent when these plants were grown on nonlimed substrate at pH 5.6 and because chlorophyll as well as Fe levels were recovered by supplying the pH-stable chelate Fe(III)-EDDHA, the defective gene was supposed to be involved in Fe acquisition. A second allelic insertion (SALK_050137C) in the same gene yielded an identical Fe-dependent phenotype (Supplemental Fig. S1, A and B).

F6′H1 Expression Is Induced in Epidermal and Cortical Cells under Fe Deficiency

The T-DNA insertion line isolated in our screen is disrupted in the expression of a gene encoding the Fe(II)- and 2-oxoglutarate-dependent dioxygenase Feruloyl-CoA 6′-Hydroxylase1 (F6′H1) (Kai et al., 2008). In the two T-DNA insertion lines used in this study, *F6′H1* expression was very low (Supplemental Fig. S2). As F6′H1 is active in the phenylpropanoid pathway and phenolic substances have been supposed to be released by Fe-deficient roots to assist Fe acquisition in various plant species (Römheld and Marschner, 1983; Jin et al., 2007; Ishimaru et al., 2011a), we investigated the Fe-dependent transcriptional regulation of *F6′H1*. In agreement with data from transcriptomics and proteomics studies of Arabidopsis roots (Dinneny et al., 2008; Buckhout et al., 2009; Lan et al., 2011), relative transcript levels of *F6′H1* increased in roots 2 to 6 d after transferring plants to Fe-deficient medium (Fig. 2C). Under Fe-sufficient conditions in the same time period, no up-regulation was observed.

To check the tissue-specific localization of *F6′H1*, transgenic seedlings expressing a *proF6′H1*:*GUS* fusion were generated. The histochemical analysis of these plants showed that *F6′H1* promoter activity was confined to roots and was up-regulated by Fe deficiency (Fig. 2A). *ProF6′H1*-dependent GUS activity was detected in the mature zone and root hair zone of primary and lateral roots but was absent in root tips (Fig. 2B). Confocal microscopy of Fe-deficient plants expressing *proF6′H1*:*F6′H1*:*GFP* fusions further revealed highest expression levels in the basal zone of the primary root, where the protein was localized in rhizodermal and cortical cells and was almost absent in Fe-sufficient plants (Fig. 2D). Increased F6′H1 levels in cortical cells were also observed in the elongation zone of primary roots of Fe-deficient plants, whereas no F6′H1-dependent GFP fluorescence was detected in primary root tips (Supplemental Fig. S3).

Fe Deficiency-Induced Synthesis and Secretion of Fluorescent Phenolics Is Dependent on F6′H1 and FIT

F6′H1 utilizes molecular oxygen to catalyze the *ortho*-hydroxylation of feruloyl-CoA, which is a prerequisite for its spontaneous isomerization and lactonization in the formation of the coumarins scopolin, scopoletin, and hydroxy-feruloyl-CoA (Kai et al., 2006, 2008). When exposed to UV light, coumarins characteristically exhibit blue fluorescence. The predominant coumarins occurring in roots of Arabidopsis are scopoletin and its glucoside scopolin, which both accumulate, particularly, under pathogen stress (Chong et al., 2002; Kai et al., 2008). In line with the function of F6′H1 in the synthesis of coumarins, the roots of *f6′h1-1* mutant plants exhibited no fluorescence under UV light at 365 nm (Fig. 3A). Importantly, root-derived fluorescence was strongly increased in wild-type plants grown under Fe deficiency. Furthermore, this fluorescence could still be detected in the agar after wild-type plants had been removed (Fig. 3A), suggesting that root-synthesized fluorescent

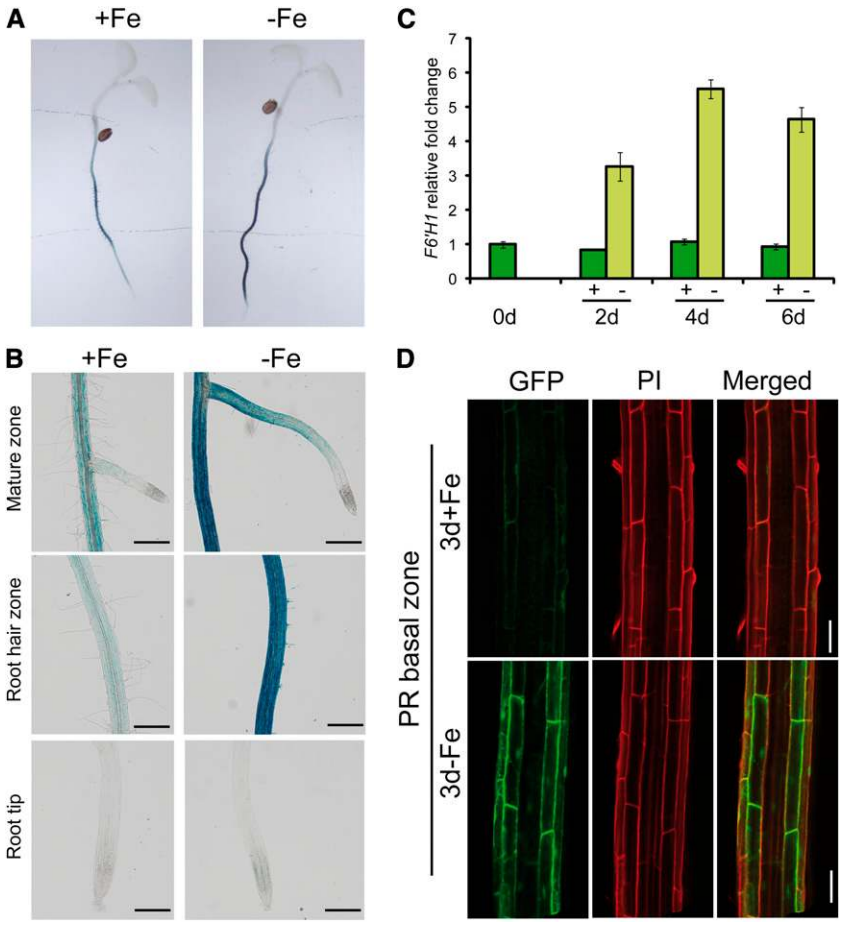

Figure 2. Relative expression level and tissue- and cell type-specific localization of *F6′H1* expression. A, Histochemical staining of GUS activity in roots of 5-d-old seedlings transformed with a translational *proF6′H1:GUS* fusion and germinated in the presence (+Fe) or absence (–Fe) of 75 μM Fe-EDTA. Images of a representative transgenic line are shown (n = 8). B, *ProF6′H1*-dependent GUS activity in different root zones of Fe-sufficient or -deficient plants. GUS activity was absent in the tips of primary and lateral roots. Plants were precultured in one-half-strength Murashige and Skoog (75 μM Fe-EDTA) medium for 5 d and then transferred to one-half-strength Murashige and Skoog medium with 75 μM Fe-EDTA (+Fe) or no Fe added plus 15 μM ferrozine (–Fe). Shown are representative root sections ($n > 10$) from one representative transgenic line. Bars = 500 μm. C, Relative expression levels of *F6′H1* in wild-type roots after transfer to an Fe-sufficient (+) or -deficient (–) medium as revealed by quantitative reverse transcription-PCR. Bars indicate means ± SE (n = five to six biological replicates). D, GFP-dependent fluorescence in epidermal and cortical cells in the basal zone of primary roots from Fe-deficient transgenic Arabidopsis plants expressing a translational F6′H1-GFP fusion under the control of its native promoter. Red fluorescence derives from propidium iodide (PI) staining of cell walls. Image of one representative transgenic line (n = 8). Bars = 50 μm.

coumarins were secreted into the medium. A closer inspection of the fluorescence pattern in the mature zone of roots revealed that fluorescence strongly increased in the outer root cells of Fe-deficient plants, colocalizing with the expression of *F6′H1* (Fig. 3D).

The Fe-dependent and cell type-specific expression pattern of *F6′H1* (Fig. 2, A, B, and D) is reminiscent to that of other genes involved in Fe acquisition, such as *IRT1* and *FRO2*, which are regulated by the bHLH-type transcription factor FIT (Colangelo and Guerinot, 2004). In fact, also, *F6′H1* up-regulation in response to Fe deficiency requires a functional FIT (Fig. 3B). Consistent with the deregulated *F6′H1* expression in the *fit* mutant, *fit* roots failed to exhibit increased accumulation of fluorescent compounds when grown under Fe deficiency (Fig. 3C). Altogether, these results suggest that F6′H1 belongs to the FIT-regulated Fe acquisition machinery in Arabidopsis roots.

Decreased Fe Mobilization Capacity of *f6′h1* Root Exudates

We then addressed the question of whether the decreased secretion of fluorescent phenolics was related to the poor ability of *f6′h1* mutants in accessing Fe under calcareous conditions (Fig. 1; Supplemental Fig. S1, A and B). Thus, we collected exudates from wild-type and *f6′h1-1* plants grown axenically with or without Fe. Then, the ability of the root exudates in mobilizing Fe(III) from freshly prepared Fe hydroxide at alkaline conditions was compared. The Fe mobilization capacity of exudates collected from both genotypes grown under sufficient Fe supply did not differ significantly (Fig. 4A). However, the exudates of Fe-deficient wild-type plants were able to mobilize 17-fold more Fe than the exudates collected from Fe-sufficient plants. Importantly, the Fe mobilization capacity of *f6′h1-1* plants grown under Fe deficiency remained low (Fig. 4A). To determine whether the Fe(III) mobilization capacity of root exudates was related to the formation of Fe complexes with catechols, we measured their formation at 460 nm (McBryde, 1964; Salama et al., 1978). When exudates from Fe-deficient wild-type plants were mixed with Fe hydroxide, significantly more Fe-catechol complexes were detected (Fig. 4B). However, it is noteworthy that the formation of Fe-catechol complexes did not completely mirror the difference in Fe(III) mobilization capacity observed when growing plants under adequate versus deficient Fe supply (Fig. 4, A and B). This suggested either that other components of the root exudates contributed to the overall Fe(III) mobilization capacity or that the absorption at 460 nm also detected other Fe complexes. As

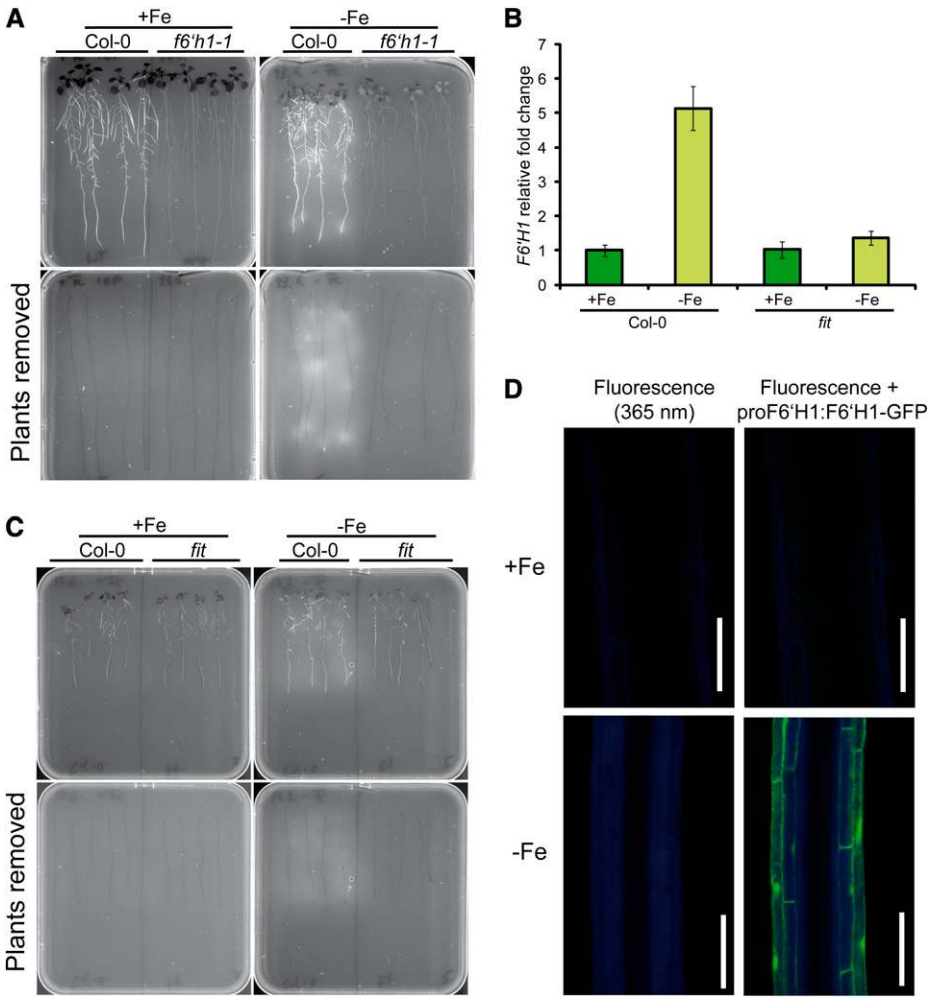

Figure 3. Accumulation of fluorescent compounds in roots and root exudates is induced by Fe deficiency. A, Top shows UV fluorescence (365 nm) in wild-type (Col-0) and *f6′h1-1* roots grown under adequate (+Fe) or deficient supply of Fe (–Fe), and bottom shows root-derived fluorescence on agar after removal of plants. B, Iron deficiency-induced *F6′H1* expression is lost in the *fit* mutant. Expression was detected in wild-type and *fit* roots 4 d after transferring to the indicated Fe regimes. Bars indicate means ± SE (*n* = five to six replicates). C, Reduced root fluorescence in Fe-deficient *fit* roots and in the agar after removal of *fit* plants. D, Blue fluorescence is induced in epidermal and cortical cells of Fe-deficient (–Fe) plants and coincides with the expression of F6′H1-GFP. Bars = 100 μm.

an approach to determine the contribution of the fluorescent compounds in the Fe(III) mobilization capacity of root exudates, we removed these compounds from the root exudates of wild-type plants by using a Sep-Pak C18 column. In fact, passing the root exudates through this column removed almost completely UV fluorescence from the exudate samples (Fig. 4C). The withdrawal of fluorescent and maybe further C18-immobilized compounds from the root exudates of Fe-deficient roots decreased significantly the Fe(III) mobilization capacity of these exudates (Fig. 4D). Altogether, these results show that the increased secretion of fluorescent phenolic compounds by Fe-deficient plants enhances the mobilization of Fe(III) from Fe hydroxide precipitates under alkaline conditions.

Fe Deficiency Induces the Exudation of Coumarins Synthesized in a F6′H1-Dependent Manner

Because *f6′h1-1* roots accumulated less fluorescent phenolic compounds and exhibited reduced Fe(III) mobilization capacity, we investigated F6′H1-dependent metabolites produced in response to Fe deficiency. We first compared the root extracts and exudates of wild-type and *f6′h1-1* plants by ultra-performance liquid chromatography (UPLC) coupled with a fluorescence detector (FLD). When compared with wild-type root extracts, several fluorescent phenolic compounds belonging to the coumarins were decreased or not detected in *f6′h1-1* extracts (Fig. 5A). In these samples, we identified scopolin as the predominant fluorescent compound in wild-type roots (Fig. 5A). Because we observed that some coumarin standards exhibit poor fluorescence under the acidic conditions used during the UPLC separation (data not shown), we extended our survey by using liquid chromatography (LC)- electrospray ionization (ESI)-mass spectrometry (MS). This approach allowed the identification of several metabolites that exhibited at least 75% reduction in *f6′h1-1* root exudates compared with the wild type under sufficient and/or deficient Fe conditions (data not shown). Although some of these metabolites could not yet be identified by our current analytical methods, we were able to identify nine of these compounds based on their mass and retention times, including scopolin,

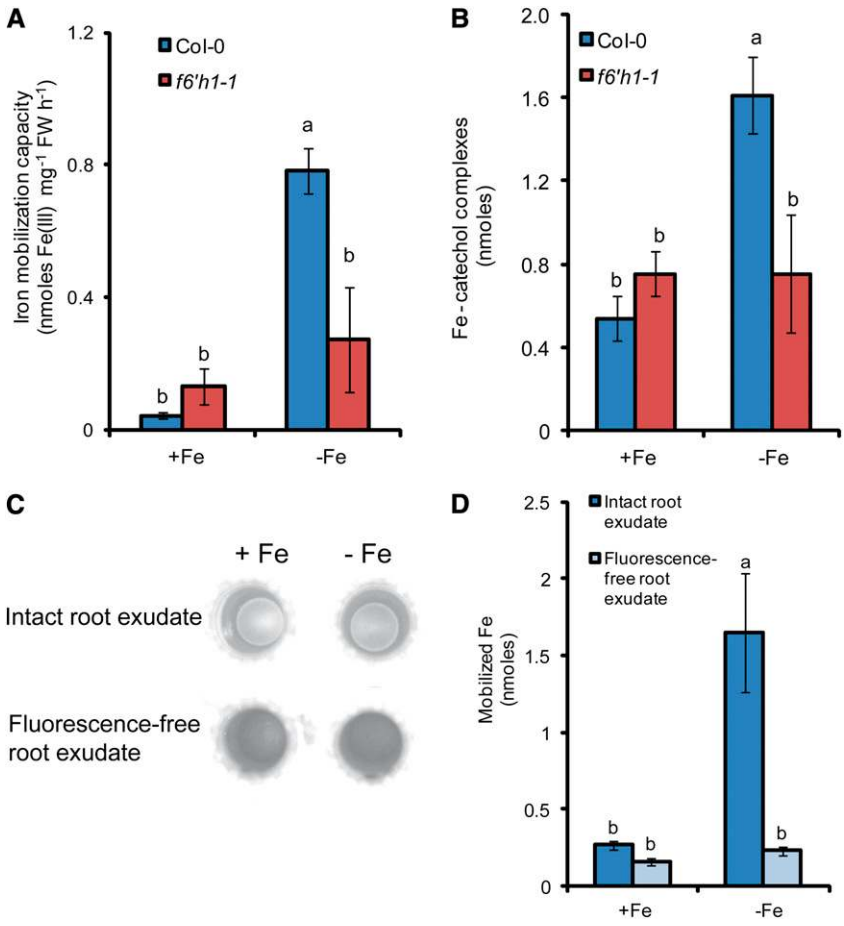

Figure 4. Fe(III) mobilization capacity of root exudates. A, Fe(III) mobilization capacity of root exudates from wild-type (Col-0) or *f6′h1-1* plants grown for 4 d in the presence (+Fe) or absence of Fe (–Fe). Exudates were incubated with precipitated Fe hydroxide at pH 7.2, and the amount of solubilized Fe was detected by high-resolution ICP-MS. B, Accumulation of Fe-catechol complexes detected at 460 nm after the incubation of root exudates with Fe hydroxide. C, Fluorescent compounds were removed from root exudates of Fe-sufficient (+Fe) or -deficient (–Fe) wild-type (Col-0) plants by passing through a Sep-Pak C18 column. D, Their Fe(III) mobilization capacity at pH 7.2 was assessed as described in A. [See online article for color version of this figure.]

scopoletin, esculin, esculetin, and fraxetin (Supplemental Table S1). We then quantified the root concentration of scopolin by LC-ESI-MS and found that it increased by approximately 40% under Fe deficiency (Fig. 5C). In roots, the concentrations of scopolin were much higher than those of its aglycon scopoletin (Fig. 5E). However, the exudation rate of scopoletin was much more pronounced than that of scopolin, exceeding it by 2-fold under Fe deficiency (Fig. 5, B, D, and F). Another prominent coumarin detected in root extracts was esculin (Fig. 5, A and G), even though it accumulated to a 500-fold lower extent than scopolin (Fig. 5, C and G). The concentration of esculin was significantly lower in *f6′h1-1* roots and even decreased in wild-type plants grown under Fe deficiency (Fig. 5G). Relative to scopolin and scopoletin, the amount of released esculin was low, irrespective of the Fe nutritional status of the plants (Fig. 5H). In quantitative terms, esculetin, the aglycon of esculin, was detected in very low amounts in roots (Fig. 5I). However, compared with its glysosylated form esculin, root exudation of esculetin was higher, increasing by 4-fold under Fe deficiency (Fig. 5, H and J). Nevertheless, the release of esculetin was by far lower than that of scopoletin (Fig. 5, F and J). In addition, the accumulation in root exudates of fraxetin, isofraxetin, and coumarins tentatively identified as isofraxidin/methoxyscopoletin was also increased in the Fe-deficient wild type but not in *f6′h1-1* plants (Supplemental Table S1). Thus, F6′H1 is required for the synthesis of several coumarins under Fe deficiency, several of which also appear in root exudates.

The Fe Deficiency-Mediated Chlorosis of *f6′h1* Can Be Rescued by the Addition of F6′H1-Dependent Coumarins

Among the identified F6′H1-dependent coumarins, esculetin was of particular interest because it accumulated in root exudates (Fig. 5J) and because it represents a dihydroxy-coumarin with adjacent hydroxy groups (Fig. 5I) resembling catechol-type siderophores (Hider and Kong, 2010). It is noteworthy that esculin and scopoletin also exhibit such a moiety but here the 6′-hydroxy position is made inaccessible by the conjugation of a glucoside or a methyl group, respectively (Fig. 5, E and G). To test whether these compounds could prevent Fe deficiency-induced chlorosis in *f6′h1-1* plants, we supplied them exogenously to plants grown under conditions where Fe availability was decreased. In the presence of exogenous esculetin, *f6′h1-1* shoots remained green and had leaf chlorophyll and Fe concentrations comparable to wild-type plants and to *f6′h1-1*

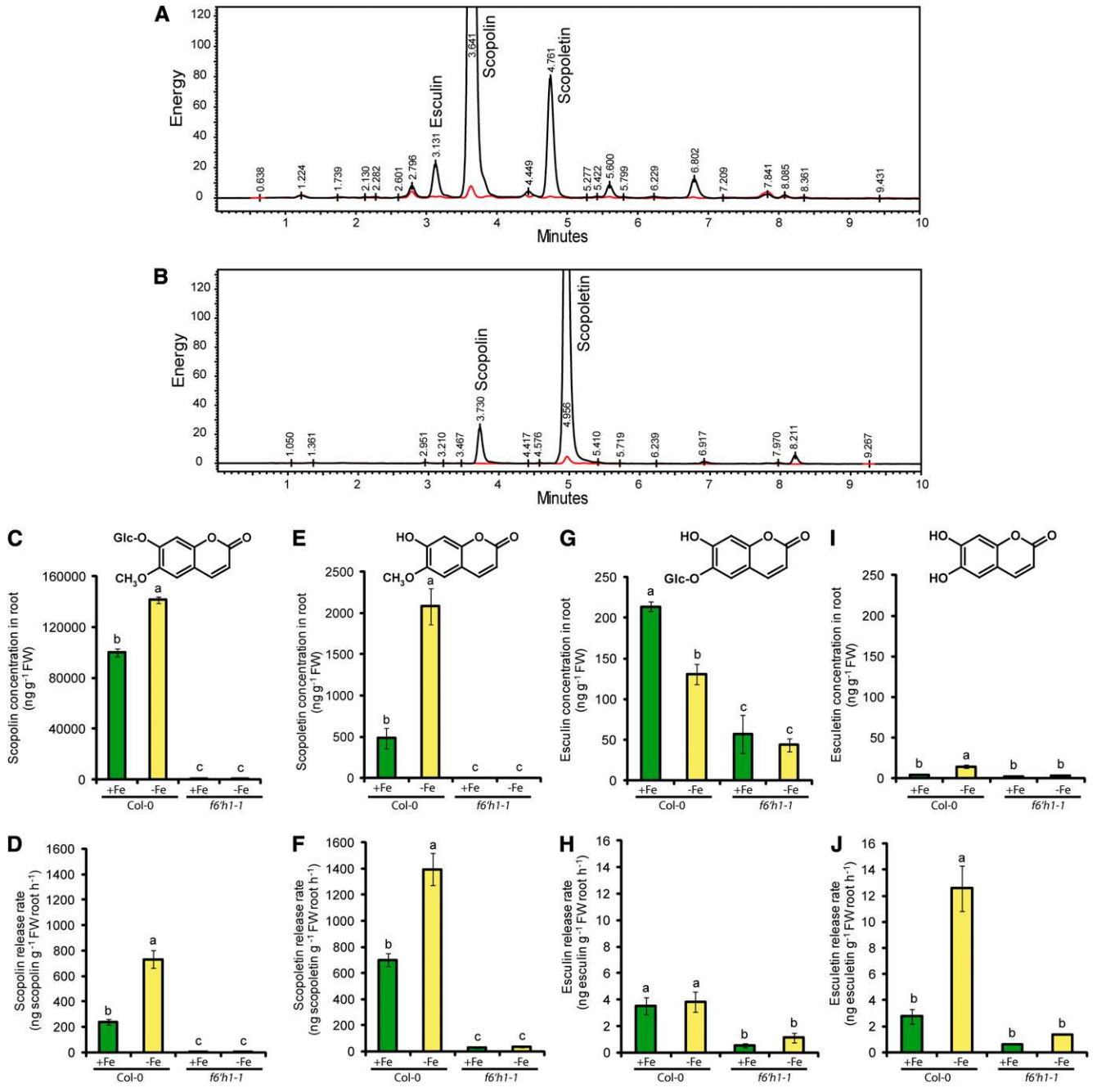

Figure 5. The accumulation of coumarins in roots and root exudates is induced by Fe deficiency. UPLC-FLD chromatograms of root extracts (A) or root exudates (B) from wild-type and *f6′h1-1* plants. Black lines indicate wild-type samples and red lines *f6′h1-1* samples. Accumulation of scopolin (C and D), scopoletin (E and F), esculin (G and H), and esculetin (I and J) in root extracts (C, E, G, and I) or root exudates (D, F, H, and J) of wild-type and *f6′h1-1* plants grown under adequate (+Fe) or deficient supply of Fe (–Fe) for 4 d. Bars indicate means ± SE (*n* = three biological replicates). Different letters indicate significant differences according to Tukey's test ($P < 0.05$).

plants supplied with EDTA (Fig. 6, A–C). Noteworthy, the ferric chelate reductase activity was not impaired in *f6′h1-1* (Supplemental Fig. S4). Interestingly, also, esculin and scopoletin prevented *f6′h1-1* plants from chlorosis and from falling below critical deficiency levels for Fe. On calcareous substrate, both esculin and esculetin were also able to rescue the chlorotic phenotype of *f6′h1-1* plants (Supplemental Fig. S1, C and D). However, when coumarins were supplied to *f6′h1-1* plants in the absence of an additional external source of Fe, they were not able to prevent the development of severe Fe deficiency symptoms in these plants (Supplemental Fig. S5). Thus,

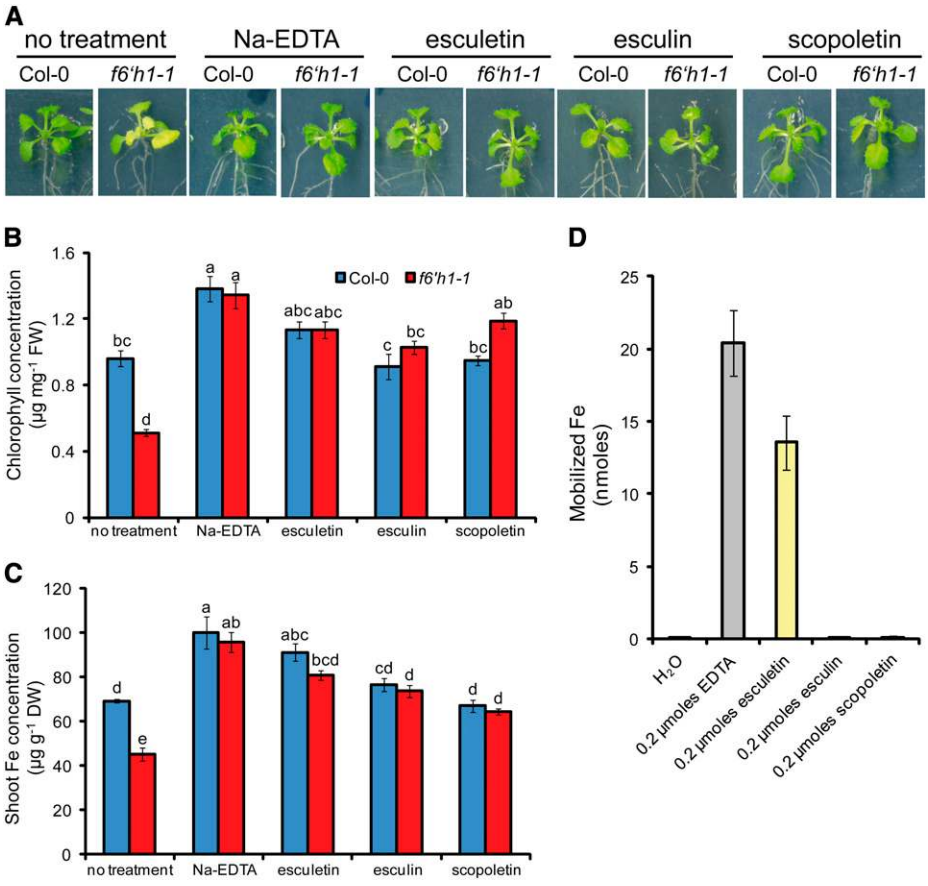

Figure 6. Coumarins prevent Fe deficiency-induced chlorosis in *f6′h1-1* plants under low Fe availability. A, Appearance of plants and the leaf concentrations of chlorophyll (B) and Fe (C) after the supply of Na-EDTA, esculetin, esculin, or scopoletin to wild-type (Col-0) and *f6′h1-1* plants grown for 6 d on low Fe availability at pH 5.6. Bars indicate means ± SE (n = five biological replicates). Letters indicate significant differences according to Tukey's test ($P < 0.05$). FW, Fresh weight; DW, dry weight. D, Fe(III) mobilization from Fe hydroxide precipitates. The indicated compounds were incubated with Fe hydroxide (pH 7.2), and the amount of solubilized Fe was detected by ICP-MS. Bars indicate means ± SE (n = 3).

these results suggest that the coumarins released by Fe-deficient plants are able to mobilize Fe from otherwise unavailable sources.

Due to a comparable efficacy of esculetin, esculin, and scopoletin in rescuing *f6′h1-1* from Fe deficiency under low Fe availability (Fig. 6, A–C), we then compared their ability to mobilize Fe(III) from Fe hydroxide at pH 7.2. As to be expected from the inaccessibility of the 6′-hydroxy group, scopoletin and esculin were incapable of mobilizing Fe(III). Only esculetin was able to chelate and mobilize Fe(III) in this in vitro assay (Fig. 6D). The Fe(III) mobilization capacity of esculetin was even comparable to that of EDTA, a potent synthetic Fe chelator.

DISCUSSION

The occurrence of Fe deficiency is a persistent problem in agricultural soils with high pH and/or high concentrations of bicarbonate, where Fe availability is strongly decreased. Because the chelator-based Fe acquisition strategy used by grasses is relatively pH insensitive, these plants can acquire Fe more efficiently under calcareous conditions, whereas the reduction-based strategy of nongraminaceous plants is strongly compromised. Early studies indicated that Fe-deficient strategy I plants not only release protons and induce a ferric chelate reductase, but also release organic compounds in the rhizosphere (Römheld and Marschner, 1981, 1983; Susín et al., 1993; Welkie, 2000). However, the importance, the mechanism of action, and the exact nature of these compounds have remained largely unknown. This work shows that the F6′H1-dependent synthesis of coumarins assists strategy I-type Fe acquisition under high pH conditions. Our results indicate that Fe-deficient Arabidopsis plants release coumarins that can chelate and mobilize Fe(III), making it available for the reduction and uptake at the plasma membrane of rhizodermal and cortical cells.

The Synthesis and Release of Coumarins Is Part of the Fe Acquisition Machinery in Arabidopsis

In a calcareous substrate that simulated the low Fe availability under alkaline soil conditions, we identified in a population of T-DNA insertion lines one mutant, *f6′h1-1*, which showed even stronger chlorosis and growth retardation than wild-type plants as a consequence of reduced Fe uptake (Fig. 1). This phenotype was not only observed when *f6′h1-1* plants were grown on solid alkaline substrate, but also when grown on agar plates with Fe being provided in an insoluble form at pH 5.6 (Fig. 6A). Noteworthy, the inability of the *f6′h1-1* mutant to acquire sparingly soluble Fe became not evident when Fe availability was sufficient, as on solid substrate at pH 5.6.

The T-DNA insertion in this mutant disrupts the expression of *F6′H1* (Supplemental Fig. S2), which encodes an enzyme previously shown to be involved in the synthesis of coumarins via the phenylpropanoid pathway (Kai et al., 2008). In agreement with early transcriptome (Colangelo and Guerinot, 2004; Dinneny et al., 2008; Yang et al., 2010; Rodríguez-Celma et al., 2013) and proteome (Lan et al., 2011) analyses, quantitative reverse transcription-PCR showed that *F6′H1* expression is strongly up-regulated in response to Fe deficiency (Fig. 2C) in a FIT-dependent manner (Fig. 3B). Because plants grown on alkaline substrate exhibited severe symptoms of Fe deficiency (Fig. 1), we assume that also other FIT-dependent genes were up-regulated under these conditions. According to the proteome study of Lan et al. (2011), Fe deficiency also induces enzymes upstream of F6′H1 in the phenylpropanoid pathway, such as PHE AMMONIA-LYASE2 and CAFFEOYL COENZYME A ESTER O-METHYLTRANSFERASE1. Furthermore, the expression of another enzyme of the phenylpropanoid pathway, TRANS-CAFFEOYL-COA 3-O-METHYLTRANSFERASE1, is also up-regulated by Fe deficiency (Fourcroy et al., 2013). These findings indicate that compounds downstream of these enzymes in the phenylpropanoid pathway, including coumarins, play an important role for the adaptation of plants to sparingly soluble Fe. This holds true whenever the Fe nutritional status of a plant is low, irrespective of whether Fe deficiency is the consequence of low Fe availability in an alkaline medium (Fig. 1), of supplying an unstable Fe source at neutral or slightly acid pH (Fig. 6), or of omitting this micronutrient from the growth medium (Fig. 3).

F6′H1 promoter activity was confined to roots (Fig. 2A) and was up-regulated by Fe deficiency especially in the basal zone of the primary root (Fig. 2B), where it mainly localized to rhizodermal and cortical cells (Fig. 2D; Supplemental Fig. S3). This Fe-dependent and cell type-specific expression pattern of *F6′H1* is reminiscent to that of other genes involved in Fe acquisition, such as *FIT* (Bauer et al., 2004; Colangelo and Guerinot, 2004), *IRT1* (Vert et al., 2002), and *FRO2* (Connolly et al., 2003). In fact, many genes encoding enzymes of the phenylpropanoid pathway, including *F6′H1*, share a similar Fe-dependent expression pattern with *FIT*, *IRT1*, *FRO2*, and *AHA2* (Rodríguez-Celma et al., 2013). Altogether, these results indicate that *F6′H1* is transcriptionally activated in roots by Fe deficiency in a FIT-dependent manner and expressed in the same root zones and cell types as other major strategy I components. Thus, F6′H1 is likely part of the FIT-regulated Fe acquisition machinery.

F6′H1 Is Required for the Synthesis of Coumarins with Fe Mobilization Capacity

F6′H1 is responsible for the conversion of feruloyl CoA to 6′-hydroxyferuloyl CoA, which serves as precursor for the synthesis of coumarins, such as scopoletin and its β-glucoside scopolin (Kai et al., 2008). Coumarins are plant-derived phenylpropanoids that originate from the precursor Phe (Bourgaud et al., 2006). The presence of these compounds in roots can be easily assessed, because many coumarins exhibit fluorescence when excited with UV light (365 nm). When the appearance of root-derived fluorescence was observed in wild-type plants, we found that fluorescence strongly increased in response to Fe deficiency (Fig. 3A) in a FIT-dependent manner (Fig. 3C). By contrast, almost no fluorescence was detected in *f6′h1-1* roots (Fig. 3A). Similar observations were recently reported in the study of Rodríguez-Celma et al. (2013). We were able to further show that the increased accumulation of fluorescent compounds under Fe deficiency coincides with an increased expression of *F6′H1* in epidermal cells (Fig. 3D). Importantly, the majority of the fluorescent compounds produced under Fe deficiency was secreted by wild-type plants (Fig. 3A). This release of fluorescent compounds under Fe deficiency is mainly mediated by the ATP-binding cassette (ABC) transporter ABCG37/PDR9 (Fourcroy et al., 2013). Because the expression of this transporter is also induced by Fe deficiency (Fourcroy et al., 2013; Rodríguez-Celma et al., 2013), in particular in rhizodermal cells (Dinneny et al., 2008; http://bbc.botany.utoronto.ca/efp), it is likely that F6′H1 and ABCG37/PDR9 work in concert to enhance the synthesis and release of fluorescent coumarins under Fe deficiency.

We then investigated the nature of the fluorescent metabolites accumulating downstream of F6′H1 under Fe deficiency. UPLC-FLD analysis showed that the accumulation not only of scopoletin and scopolin but also of other coumarins was significantly decreased in *f6′h1-1* roots (Fig. 5A). A more exploratory UPLC-ESI-MS analysis revealed that several compounds were increased in wild-type roots under Fe deficiency but remained relatively low in *f6′h1-1* roots (Supplemental Table S1). These results indicated that F6′H1 is a key enzyme not only for the synthesis of scopolin and scopoletin as shown by Kai et al. (2008), but also for other less abundant coumarins, such as esculetin (Fig. 5). Although scopolin was the most abundant coumarin in roots, its aglycon scopoletin was the prevailing compound in root exudates (Fig. 5, A–F). Possibly, the higher accumulation of scopolin in roots helps to overcome the low solubility of its aglycon scopoletin and protects it from intracellular oxidation (Chong et al., 1999). In addition, because scopoletin was more abundant in root exudates, it is likely that scopolin undergoes deglycosylation just before or right after being exported across the root plasma membrane. This assumption is in agreement with the existence of root-expressed β-glucosidases that have the capacity to hydrolyze scopolin (Ahn et al., 2010). Interestingly, such a modification is not restricted to the pair scopolin-scopoletin but may also apply to esculin and its aglycon esculetin. While esculin was more abundant in roots, esculetin was rather detected in root exudates (Fig. 5, G–J). Similar to scopoletin, further chemical modifications in the root apoplast may be involved in the enrichment of esculetin in root exudates, because esculin can also serve as

substrate for root-expressed β-glucosidases (Ahn et al., 2010).

Because most of the F6′H1-dependent coumarins were released into the growth medium under Fe deficiency (Supplemental Table S1), it is likely that they play a functional role outside the root cells. Employing mobilization assays that reflect a chelator-dependent dissolution of Fe hydroxide, we observed that Fe deficiency increased the Fe(III) mobilization capacity of root exudates from wild-type plants, whereas such an increase was almost completely absent when the assay was carried out with *f6′h1-1* root exudates (Fig. 4A). Furthermore, when fluorescent compounds were removed from root exudates of Fe-deficient wild-type plants (Fig. 4C), the Fe(III) mobilization capacity of these exudates strongly decreased (Fig. 4D). Because the Sep-Pak C18 resin was washed three times with 10% (v/v) methanol, we assume that most organic acids that could also chelate Fe(III) were separated from the fluorescent compounds and did not substantially contribute to Fe mobilization (Fig. 4, C and D). Thus, one or more of the coumarins synthesized in an F6′H1-dependent manner must be able to chelate and solubilize Fe from Fe-hydroxide precipitates. Importantly, our Fe(III) mobilization assays were performed at high pH, indicating that Fe(III) mobilization and chelation by coumarins is not sensitive to alkaline pH. Although some phenolics are also able to reduce Fe(III), the efficiency of this reaction is significantly decreased under high pH (Römheld and Marschner, 1983; Mladenka et al., 2010). Thus, we assume that Fe(III) reduction by coumarins may not be relevant under alkaline conditions. Although the chemical identity of the root exudate compounds conferring Fe mobilization capacity could not yet be completely resolved, a part of the resulting Fe(III) complexes formed in the mobilization assay showed absorption at 460 nm (Fig. 4B), which is indicative for Fe-catechol complexes (McBryde, 1964; Salama et al., 1978). In fact, not only coumarins, but also other phenols have been shown to chelate Fe(III) in vitro if they contain two adjacent hydroxy groups (catechol moiety; Andjelkovic et al., 2006; Mladenka et al., 2010). Among the coumarins identified in this study, esculetin and fraxetin harbor such a moiety, whereas in others, the hydroxy group is either methylated (scopoletin; Fig. 1E) or engaged in a glycosidic linkage (esculin; Fig. 1G). Although Fe(III) mobilization by coumarins is relatively pH insensitive (Fig. 4A), wild-type plants still suffered from Fe deficiency when grown on high pH conditions (Fig. 1A). This might indicate that Fe(III) reduction via the ferric-chelate reductase was then the rate-limiting step for Fe acquisition under these conditions.

Esculetin as a Prototype for Fe(III)-Mobilizing Catechols Secreted by Fe-Deficient Arabidopsis Roots

The supply of scopoletin, esculin, and esculetin to agar-grown *f6′h1-1* plants prevented the development of Fe deficiency symptoms in these plants (Fig. 6, A–C). We exclude here an indirect mode of action of these coumarins, such as via the involvement of microbial Fe(III) dissolution, because plants were kept under axenic conditions (Fig. 6, A–C). Because the chlorotic phenotype of *f6′h1-1* plants could not be rescued if there was no Fe available in the growth medium (Supplemental Fig. S5), the supplied coumarins apparently did not remobilize Fe from the root apoplast or another plant-endogenous pool. Instead, their effectiveness depended on the presence of an external Fe source, supporting a crucial role of the released coumarins in Fe mobilization from the rhizosphere. Although esculetin, esculin, and scopoletin prevented *f6′h1-1* plants from Fe deficiency-induced chlorosis (Fig. 6, A–C; Supplemental Fig. S1), only esculetin was able to mobilize Fe(III) from precipitated Fe hydroxide in vitro (Fig. 6D). Esculetin (i.e. 6,7-dihydroxycoumarin) is a simple coumarin that harbors two adjacent hydroxy groups in the 5′- and 6′-position of the benzene ring (Fig. 5I). This particular structure resembles that of catechol-type siderophores produced and released by bacteria or fungi to mobilize and chelate Fe (Hider and Kong, 2010). Interestingly, some bacteria do not synthesize but utilize esculetin as exogenous siderophore to acquire Fe (Coulanges et al., 1996). In this case, microorganisms produce esculetin mainly from the hydrolysis of plant-derived esculin. In addition, esculetin has been described to occur in soils as an oxidation product of caffeic acid (Deiana et al., 1995). However, we were not able to detect caffeic acid in root exudates (data not shown). Instead, we propose a conversion of released coumarins in the root apoplast, in a way that esculetin derived from the deglycosylation of esculin or the demethylation of scopoletin could act as one of the F6′H1-dependent fluorescent coumarins that was effective in Fe(III) mobilization. This may also explain why esculin and scopoletin were able to alleviate Fe deficiency symptoms in *f6′h1-1* plants even though they are not capable of mobilizing insoluble Fe per se. As the catechol moiety of esculetin is unhindered, two adjacent oxygen atoms become competent in the formation of coordinative bondings with Fe(III), thereby fulfilling the requirements for successful chelation. In general, Fe(III) catechol complex formation occurs over a wide pH range up to 9 (Powell and Taylor, 1982) and is thus capable of Fe(III) chelation in alkaline soils.

Our findings indicate that the induction of F6′H1 by Fe deficiency leads to the synthesis of coumarins secreted from roots. Once in the rhizosphere, some of these coumarins may undergo modifications to become effective Fe(III) chelators such as esculetin. So far, we cannot yet quantify to which extent the Fe(III) mobilization capacity of root exudates from Fe-deficient Arabidopsis plants is caused by esculetin. Therefore, future challenges are to determine the nature of the remaining unknown coumarins, which could not yet be identified by our LC-ESI-MS method, and to develop approaches for a direct comparison of Fe(III) mobilization capacities of individual root exudate components.

MATERIALS AND METHODS

Plant Materials and Growth Conditions

In this study, we used the Arabidopsis (*Arabidopsis thaliana*) accession line Columbia (Col-0) as the wild type. The following T-DNA insertion and mutant lines in the Col-0 genetic background were used: *f6′h1-1* (At3g13610; SALK_132418C), *f6′h1-2* (At3g13610; SALK_050137C), and *fit* (At2g28160; *fit-3* allele; Jakoby et al., 2004). To screen for mutants with reduced ability to acquire Fe from soils with high pH, 3,500 homozygous T-DNA insertion lines (Alonso et al., 2003) were grown on peat-based substrate ('Klasmann Substrat 1'). The pH of the substrate was either maintained at pH 5.6 or increased to pH 7.2 by the supplementation of 20 g kg^{-1} $CaCO_3$ and 12 g kg^{-1} $NaHCO_3$. Each insertion mutant was grown on substrate pH 5.6 and 7.2 (n = three replicates). Plants were cultivated in 54 pot trays, on which three wild-type (Col-0) plants were included. The trays were placed inside a conditioned growth chamber with a 22°C/18°C and 9-h/15-h light/dark regime at a light intensity of 120 to 150 μmol photons m^{-2} s^{-1}. The screen consisted of visually assessing the appearance and intensity of Fe deficiency symptoms (e.g. chlorosis in young leaves) in insertion lines grown at pH 7.2 compared with both the same insertion line grown on pH 5.6 or wild-type plants grown on pH 7.2. Additional experiments on peat substrate were carried out as described above for 17 d. Depending on the experiment, 2.0 mL of a 4.4 g L^{-1} Fe-sequestrene (6% Fe(III)-EDDHA, Syngenta), 29 mM esculin (Roth), or 34 mM esculetin (Roth) were supplied two to three times during 4 d to assess whether these compounds could alleviate Fe deficiency symptoms of plants.

In experiments with agar plates, seeds were surface sterilized with a solution containing 70% (v/v) ethanol and 0.05% (v/v) Triton X-100. Seeds were then sown on sterile plates containing one-half-strength Murashige and Skoog medium (Murashige and Skoog, 1962) with 40 or 75 μM Fe-EDTA, supplemented with 0.5% Suc, 2.5 mM MES (pH 5.6 or 7.2), and 1% (w/v) Difco agar (Becton Dickinson). The plates were incubated at 4°C for 2 d to synchronize seed germination. Afterward, the agar plates were kept in a vertical position inside growth cabinets under a 22°C/18°C and 10-h/14-h light/dark regime with light intensity adjusted to 120 μmol photons m^{-2} s^{-1}. After 8 to 10 d, seedlings were transferred to various treatments, depending on the experiment. The agar plates contained a one-half-strength Murashige and Skoog medium supplemented or not with Fe (see figure legends). When investigating the effect of different coumarins on preventing Fe deficiency, the following conditions were used: the pH of one-half-strength Murashige and Skoog agar medium was adjusted to 5.6 or 7.2 by KOH and buffered by 2.5 mM MES. Fe was supplemented as a poorly available form (50 μM $FeCl_3$). These plates received either no additional treatment (no treatment) or were supplemented with 160 μM Na-EDTA, 500 μM esculetin (Roth), or 500 or 50 μM scopoletin (Sigma Aldrich). Plants were assessed after 6 d on these conditions.

Imaging, Scanning, and Fluorescence Imaging of Plants

Photographs of plants grown on substrate were taken with a Canon Digital IXUS 70, maintaining the same settings in manual modus. Plants grown on agar plates were scanned by an Epson Expression 10000XL scanner at a resolution of 300 dots per inch. Root fluorescence was imaged by a fluorescence imaging system Quantum ST4 (Vilber Lourmat). Excitation was adjusted by epi-UV at 365 nm, and the light emitted was filtered by a 440-nm filter (F–440M58). The images were taken with the help of the Quantum-capt version 15.17 software.

Chlorophyll and Shoot Fe Determination

Whole shoot samples were incubated at 4°C for 24 h in *N*,*N*′-dimethyl formamide (Merck). The A_{647} and A_{664} was then determined in the extracts following the protocol described by Porra et al. (1989). For Fe measurements, whole shoot samples were dried for 48 h at 65°C and digested with HNO_3 in polytetrafluoroethylene vials in a pressurized microwave digestion system (UltraCLAVE IV, MLS GmbH). Iron concentrations were analyzed by inductively coupled plasma (ICP)-optical emission spectrometry (iCAP 6500 Dual OES Spectrometer, Thermo Fischer Scientific).

Cloning and Plant Transformation

A 3,230-bp fragment containing the *F6′H1* promoter (2,064 bp) and open reading frame region was amplified from the genomic DNA of Arabidopsis (accession Col-0) plants using the primers indicated in Supplemental Table S2. Genomic DNA was extracted according to the instructions of the DNeasy Plant Mini Kit from Qiagen. The Phusion High-Fidelity DNA Polymerase (Finnzymes; Thermo Fisher Scientific) was used for amplification. To study the tissue localization of *F6′H1* expression via GUS, the 2,064-bp promoter region of *F6′H1* was amplified from genomic DNA using the primers listed in Supplemental Table S2. In both cases, the resulting amplicons were cloned into the pENTR/TOPO entry vector following the manufacturer's instruction (Invitrogen) and then subcloned into the Gateway plant expression vector pGWB4 (no promoter, C-sGFP) or pGWB3 vector (no promoter, C-GUS) by the recombination of attL and attR sites. The *Agrobacterium tumefaciens* strain C58C1 (pGV2260) was used to transform wild-type (Col-0) plants with these binary vectors according to the floral dip protocol (Clough and Bent, 1998). Plant transformants were selected on agar medium containing kanamycin. For each transgenic construct, at least eight independent lines were analyzed.

Histochemical and Microscopy Analyses

The tissue localization of *F6′H1* was determined by histochemical staining of the GUS activity in Arabidopsis seedlings transformed with the construct *ProF6′H1-1:GUS* following the protocol described in Giehl et al. (2012). At least 10 seedlings per independent transgenic line and treatment were analyzed. GFP-dependent fluorescence in roots of *ProF6′H1-1-F6′H1-1-GFP* lines was detected with a confocal microscope LSM 510 Meta (Carl Zeiss MicroImaging GmbH). Roots were stained with propidium iodide (10 μg mL^{-1}) for 10 min. GFP-dependent fluorescence was detected by excitation at 488 nm with an argon laser and filtering the emitted light at 505 to 530 nm. The 488-nm excitation and 458- to 514-nm emission lines were used to image the propidium iodide-derived fluorescence. The software LSM 510 release 3.2 (Zeiss) was used for adjustments and image recording.

Gene Expression Analysis

Plants were grown axenically on agar plates, and total RNA was extracted from roots of either Fe-sufficient or -deficient Col-0 or *fit* mutant plants using a modified version of the single-step method (Chomczynski and Sacchi, 1987). For reverse transcription of RNA into complementary DNA, the RevertAid First Strand cDNA Synthesis Kit of Fermentas was used using oligo(dT)-primers and RNA samples treated previously with RQ1 RNase-Free DNase (Promega). The complementary DNA samples were then used to investigate gene expression by quantitative real-time PCR with the Mastercycler ep realplex (Eppendorf) and the iQ SYBR Green Supermix (Bio-Rad Laboratories) using the primers listed in Supplemental Table S2. Relative expression was calculated according to Pfaffl (2001).

Collection of Root Exudates and Root Extractions

Root exudates were collected from 14-d-old plants grown axenically for 4 d on Fe-sufficient (75 μM Fe-EDTA) or -deficient (no added Fe + 50 μM ferrozine) solid media. The plants were carefully transferred from the agar plates to a 12-well plate (12 plants per well) containing 5 mL of ultrapure water per well (Millipore). The well pates were placed inside bowls covered with polyvinyl chloride film to prevent dehydration. The trays were kept under 22°C, with constant illumination (120 μmol photons m^{-2} s^{-1}). After 6 h, the water solution containing the root exudates was collected. The exudates of approximately 144 plants were combined as one replicate. These solutions were concentrated in a rotary evaporator (Rotavapor R-210/215, Büchi). Evaporated samples were then resuspended in 10 mL 100% methanol and sonicated for 5 min and finally concentrated to 0.5 mL using a Christ ALPHA RVC centrifugal evaporator. In the case of fluorescence-free root exudates, the complete exudates were loaded on a Sep-Pak C18 catridge (Water). The column was washed three times with 10% (v/v) methanol, and the combined fluorescence-free flow-through and wash solution was used for Fe(III) mobilization.

To extract phenolic compounds from roots, 100% methanol was added to frozen root samples (400 μL methanol per 100 mg roots), and the samples were homogenized using a tissue homogenizer (Precellys 24, Bertin Technologies) and zirconium silicate (58%) grinding beads (diameter, 1–1.2 mm; RIMAX ZS-R, Mühlmeier GmbH) for 2 × 45 s at 5,500 rpm. After centrifugation (16,400 rpm/28,500g, at 4°C for 10 min), the supernatant was transferred into a new tube, the pellet was resuspended again with the same amount of methanol, and the second supernatant was combined with the first. An aliquot of this sample was then diluted to 80% with the acidic solvent from the aqueous phase of the HPLC before injection (Korn et al., 2008).

Fe Mobilization Assays

Iron mobilization capacity was determined by incubating different compounds or root exudates with freshly prepared 0.1 mM Fe hydroxide at pH 7.2. Samples were incubated at constant shaking for 2 h. Afterwards, the solutions were filtered by Chromafil CA-45/25 (0.45-μm pore) filters. The Fe concentrations in the filtrates were detected by sector field high-resolution ICP-MS (ELEMENT 2, Thermo Fisher Scientific). Element standards were prepared from certified reference single standards from CPI International. ^{56}Fe was used as external standard and ^{103}Rh as internal standard for matrix correction. The ICP multielement standard solution VI (Merck) was used for quality control.

Determination of Coumarins in Root Extracts and Exudates by UPLC-FLD

Root extracts and exudates were subjected to separation by a Waters Acquity UPLC system fitted with an Acquity UPLC photodiode array detector and an Acquity UPLC FLD. This separation method followed the protocol described by Yonekura-Sakakibara et al. (2008). Briefly, the Waters Acquity UPLC system was equipped with an Acquity UPLC BEH Phenyl Column (130Å, 2.1 × 100 mm, 1.7 μm) and an Acquity UPLC BEH Phenyl VanGuard Precolumn (130Å, 2.1 × 5 mm, 1.7 μm). The column temperature was set to 35°C. The gradient was linear from 0 min, 100% solvent A (0.1% [v/v] formic acid in 18-mΩ water [Milli-Q]), to 10 min, 40% B (0.1% [v/v] formic acid in acetonitrile). Solvent B was brought up to 100% after each run to clean the column, and the initial conditions were restored in a delay of 3.5 min. Samples were evaluated with UV detection at 280 nm and fluorescence detection at 300/400 nm, 336/438 nm, and 360/450 nm.

Determination of Coumarin Concentrations in Root Extracts and Exudates via UPLC-ESI-MS

UPLC-ESI-time-of-flight was carried out with a Dionex Ultimate 3000 UPLC system (Thermo Fisher Scientific) coupled to an ultra-high-resolution time-of-flight mass spectrometer (maXis impact, Bruker Daltonics). The HPLC conditions were those as described above. ESI was carried out in positive mode. MS settings were optimized for small to medium molecules established on the coumarin standards esculin, esculetin, scopolin, and scopoletin (mass range, 50–1,000 mass-to-charge ratio; capillary voltage, 4,000 V; nebulizer, 3 bar; dry gas, 11 L min^{-1}; dry temperature, 260°C; hexapole radio frequency voltage (RF), 40 volts, peak-to-peak (Vpp); funnel 1 RF, 300 Vpp; funnel 2 RF, 300 Vpp; prepulse storage time, 5 μs; transfer time, 50 μs; low mass, 40 mass-to-charge ratio; collision cell RF, 500 Vpp; and collision energy, 8 eV). Calibration was performed externally before each run with 10 mM sodium formate, using the calibration mode "quadratic + HPC (for High Precision Calibration)." Data analysis was carried out with Compass DataAnalysis V.4.1 and Compass QuantAnalysis V2.1 (Bruker Daltonik GmbH).

Supplemental Data

The following materials are available in the online version of this article.

Supplemental Figure S1. Phenotypical analysis of a second independent T-DNA insertion line of F6′H1.

Supplemental Figure S2. *F6′H1* expression in the two T-DNA insertion lines used in this study.

Supplemental Figure S3. Cell type-specific localization of F6′H1 expression.

Supplemental Figure S4. Ferric reductase activity assay in roots of wild-type (Col-0) and *f6′h1-1* mutant plants.

Supplemental Figure S5. Esculetin and scopoletin cannot prevent Fe deficiency-induced chlorosis in the absence of an external Fe source.

Supplemental Table S1. Compounds identified in the root exudates of wild-type (Col-0) and *f6′h1-1* plants.

Supplemental Table S2. List of primers used in the study.

ACKNOWLEDGMENTS

We thank Dr. Swetlana Friedel, Dr. Twan Rutten, Elis Fraust, Melanie Ruff, Susanne Reiner, Andrea Knospe, and Heike Nierig (Leibniz Institute for Plant Genetics and Crop Plant Research) for excellent assistance and Tsuyoshi Nakagawa (Research Institute of Molecular Genetics, Shimane University) for the plant expression vectors pGWB3 and pGWB4.

Received September 14, 2013; accepted November 14, 2013; published November 18, 2013.

LITERATURE CITED

Ahn YO, Shimizu B, Sakata K, Gantulga D, Zhou C, Bevan DR, Esen A (2010) Scopolin-hydrolyzing β-glucosidases in roots of Arabidopsis. Plant Cell Physiol **51:** 132–143

Alcantara E, Romera FJ, Canete M, de la Guardia MD (2000) Effects of bicarbonate and iron supply on Fe(III) reducing capacity of roots and leaf chlorosis of the susceptible peach rootstock "Nemaguard." J Plant Nutr **23:** 1607–1617

Alonso JM, Stepanova AN, Leisse TJ, Kim CJ, Chen H, Shinn P, Stevenson DK, Zimmerman J, Barajas P, Cheuk R, et al (2003) Genome-wide insertional mutagenesis of *Arabidopsis thaliana*. Science **301:** 653–657

Andjelkovic M, Van Camp J, De Meulenaer B, Depaemelaere G, Socaciu C, Verloo M, Verhe R (2006) Iron-chelation properties of phenolic acids bearing catechol and galloyl groups. Food Chem **98:** 23–31

Bauer P, Jakoby M, Wang HY, Reidt W, Weisshaar B (2004) FRU (BHLH029) is required for induction of iron mobilization genes in *Arabidopsis thaliana*. Febs Letters **577:** 528–534

Beinert H, Holm RH, Münck E (1997) Iron-sulfur clusters: nature's modular, multipurpose structures. Science **277:** 653–659

Bourgaud F, Hehn A, Larbat R, Doerper S, Gontier E, Kellner S, Matern U (2006) Biosynthesis of coumarins in plants: a major pathway still to be unravelled for cytochrome P450 enzymes. Phytochem Rev **5:** 293–308

Buckhout TJ, Yang TJW, Schmidt W (2009) Early iron-deficiency-induced transcriptional changes in Arabidopsis roots as revealed by microarray analyses. BMC Genomics **10:** 147

Carvalhais LC, Dennis PG, Fedoseyenko D, Hajirezaei MR, Borriss R, von Wirén N (2011) Root exudation of sugars, amino acids, and organic acids by maize as affected by nitrogen, phosphorus, potassium, and iron deficiency. J Plant Nutr Soil Sci **174:** 3–11

Chen Y, Barak P (1982) Iron nutrition of plants in calcareous soils. Adv Agron **35:** 217–240

Chomczynski P, Sacchi N (1987) Single-step method of RNA isolation by acid guanidinium thiocyanate-phenol-chloroform extraction. Anal Biochem **162:** 156–159

Chong J, Baltz R, Fritig B, Saindrenan P (1999) An early salicylic acid-, pathogen-, and elicitor-inducible tobacco glucosyltransferase: role in compartmentalization of phenolics and H_2O_2 metabolism. FEBS Lett **458:** 204–208

Chong J, Baltz R, Schmitt C, Beffa R, Fritig B, Saindrenan P (2002) Downregulation of a pathogen-responsive tobacco UDP-Glc:phenylpropanoid glucosyltransferase reduces scopoletin glucoside accumulation, enhances oxidative stress, and weakens virus resistance. Plant Cell **14:** 1093–1107

Clough SJ, Bent AF (1998) Floral dip: a simplified method for *Agrobacterium*-mediated transformation of *Arabidopsis thaliana*. Plant J **16:** 735–743

Colangelo EP, Guerinot ML (2004) The essential basic helix-loop-helix protein FIT1 is required for the iron deficiency response. Plant Cell **16:** 3400–3412

Connolly EL, Campbell NH, Grotz N, Prichard CL, Guerinot ML (2003) Overexpression of the FRO2 ferric chelate reductase confers tolerance to growth on low iron and uncovers posttranscriptional control. Plant Physiol **133:** 1102–1110

Coulanges V, André P, Vidon DJM (1996) Esculetin antagonizes iron-chelating agents and increases the virulence of *Listeria* monocytogenes. Res Microbiol **147:** 677–685

Curie C, Panaviene Z, Loulergue C, Dellaporta SL, Briat JF, Walker EL (2001) Maize yellow stripe1 encodes a membrane protein directly involved in Fe(III) uptake. Nature **409:** 346–349

Deiana S, Gessa C, Pilo MI, Premoli A, Solinas V (1995) Role of the caffeic acid oxidation products on the iron mobilization at the soil-root interface. Plant Biosyst **129:** 941–942

Dinneny JR, Long TA, Wang JY, Jung JW, Mace D, Pointer S, Barron C, Brady SM, Schiefelbein J, Benfey PN (2008) Cell identity mediates the response of Arabidopsis roots to abiotic stress. Science **320:** 942–945

Eide D, Broderius M, Fett J, Guerinot ML (1996) A novel iron-regulated metal transporter from plants identified by functional expression in yeast. Proc Natl Acad Sci USA **93:** 5624–5628

Fourcroy P, Sisó-Terraza P, Sudre D, Savirón M, Reyt G, Gaymard F, Abadía A, Abadia J, Alvarez-Fernández A, Briat JF (2013) Involvement of the ABCG37 transporter in secretion of scopoletin and derivatives by Arabidopsis roots in response to iron deficiency. New Phytol

Giehl RFH, Lima JE, von Wirén N (2012) Localized iron supply triggers lateral root elongation in *Arabidopsis* by altering the AUX1-mediated auxin distribution. Plant Cell **24:** 33–49

Giehl RFH, Meda AR, von Wirén N (2009) Moving up, down, and everywhere: signaling of micronutrients in plants. Curr Opin Plant Biol **12:** 320–327

Hider RC, Kong X (2010) Chemistry and biology of siderophores. Nat Prod Rep **27:** 637–657

Ishimaru Y, Bashir K, Nakanishi H, Nishizawa NK (2011a) The role of rice phenolics efflux transporter in solubilizing apoplasmic iron. Plant Signal Behav **6:** 1624–1626

Ishimaru Y, Kakei Y, Shimo H, Bashir K, Sato Y, Sato Y, Uozumi N, Nakanishi H, Nishizawa NK (2011b) A rice phenolic efflux transporter is essential for solubilizing precipitated apoplasmic iron in the plant stele. J Biol Chem **286:** 24649–24655

Jakoby M, Wang HY, Reidt W, Weisshaar B, Bauer P (2004) FRU (BHLH029) is required for induction of iron mobilization genes in *Arabidopsis thaliana*. FEBS Lett **577:** 528–534

Jin CW, You GY, He YF, Tang C, Wu P, Zheng SJ (2007) Iron deficiency-induced secretion of phenolics facilitates the reutilization of root apoplastic iron in red clover. Plant Physiol **144:** 278–285

Kai K, Mizutani M, Kawamura N, Yamamoto R, Tamai M, Yamaguchi H, Sakata K, Shimizu B (2008) Scopoletin is biosynthesized via ortho-hydroxylation of feruloyl CoA by a 2-oxoglutarate-dependent dioxygenase in *Arabidopsis thaliana*. Plant J **55:** 989–999

Kai K, Shimizu B, Mizutani M, Watanabe K, Sakata K (2006) Accumulation of coumarins in *Arabidopsis thaliana*. Phytochemistry **67:** 379–386

Kim SA, Guerinot ML (2007) Mining iron: iron uptake and transport in plants. FEBS Lett **581:** 2273–2280

Kobayashi T, Nishizawa NK (2012) Iron uptake, translocation, and regulation in higher plants. Annu Rev Plant Biol **63:** 131–152

Korn M, Peterek S, Mock HP, Heyer AG, Hincha DK (2008) Heterosis in the freezing tolerance, and sugar and flavonoid contents of crosses between *Arabidopsis thaliana* accessions of widely varying freezing tolerance. Plant Cell Environ **31:** 813–827

Lan P, Li W, Wen TN, Shiau JY, Wu YC, Lin W, Schmidt W (2011) iTRAQ protein profile analysis of Arabidopsis roots reveals new aspects critical for iron homeostasis. Plant Physiol **155:** 821–834

Lemanceau P, Bauer P, Kraemer S, Briat JF (2009) Iron dynamics in the rhizosphere as a case study for analyzing interactions between soils, plants and microbes. Plant Soil **321:** 513–535

Lucena C, Romera FJ, Rojas CL, Garcia M, Alcantara E, Perez-Vicente R (2007) Bicarbonate blocks the expression of several genes involved in the physiological responses to Fe deficiency of Strategy I plants. Funct Plant Biol **34:** 1002–1009

Marschner P (2012) Marschner's Mineral Nutrition of Higher Plants, Ed 3. Academic Press, San Diego

Massé E, Arguin M (2005) Ironing out the problem: new mechanisms of iron homeostasis. Trends Biochem Sci **30:** 462–468

McBryde WAE (1964) A spectrophotometric reexamination of the spectra and stabilities of the iron (III)-tiron complexes. Can J Chem **42:** 1917–1927

Mladenka P, Macáková K, Zatloukalová L, Reháková Z, Singh BK, Prasad AK, Parmar VS, Jahodár L, Hrdina R, Saso L (2010) In vitro interactions of coumarins with iron. Biochimie **92:** 1108–1114

Murashige T, Skoog F (1962) A revised medium for rapid growth and bio assays with tobacco tissue cultures. Physiol Plant **15:** 473–497

Nozoye T, Nagasaka S, Kobayashi T, Takahashi M, Sato Y, Sato Y, Uozumi N, Nakanishi H, Nishizawa NK (2011) Phytosiderophore efflux transporters are crucial for iron acquisition in graminaceous plants. J Biol Chem **286:** 5446–5454

Ohwaki Y, Sugahara K (1997) Active extrusion of protons and exudation of carboxylic acids in response to iron deficiency by roots of chickpea (*Cicer arietinum* L). Plant Soil **189:** 49–55

Peiffer GA, King KE, Severin AJ, May GD, Cianzio SR, Lin SF, Lauter NC, Shoemaker RC (2012) Identification of candidate genes underlying an iron efficiency quantitative trait locus in soybean. Plant Physiol **158:** 1745–1754

Pfaffl MW (2001) A new mathematical model for relative quantification in real-time RT-PCR. Nucleic Acids Res **29:** e45

Porra RJ, Thompson WA, Kriedemann PE (1989) Determination of accurate extinction coefficients and simultaneous equations for assaying chlorophyll-*a* and chlorophyll-*b* extracted with 4 different solvents: verification of the concentration of chlorophyll standards by atomic-absorption spectroscopy. Biochim Biophys Acta **975:** 384–394

Powell H, Taylor M (1982) Interactions of iron(II) and iron(III) with gallic acid and its homologues: a potentiometric and spectrophotometric study. Aust J Chem **35:** 739–756

Robinson NJ, Procter CM, Connolly EL, Guerinot ML (1999) A ferric-chelate reductase for iron uptake from soils. Nature **397:** 694–697

Rodríguez-Celma J, Lin WD, Fu GM, Abadía J, López-Millán AF, Schmidt W (2013) Mutually exclusive alterations in secondary metabolism are critical for the uptake of insoluble iron compounds by Arabidopsis and *Medicago truncatula*. Plant Physiol **162:** 1473–1485

Rodríguez-Celma J, Vázquez-Reina S, Orduna J, Abadía A, Abadía J, Álvarez-Fernández A, López-Millán AF (2011) Characterization of flavins in roots of Fe-deficient strategy I plants, with a focus on *Medicago truncatula*. Plant Cell Physiol **52:** 2173–2189

Romera FJ, Alcantara E, delaGuardia MD (1997) Influence of bicarbonate and metal ions on the development of root Fe(III) reducing capacity by Fe-deficient cucumber (*Cucumis sativus*) plants. Physiol Plant **101:** 143–148

Römheld V, Marschner H (1981) Iron-deficiency stress induced morphological and physiological changes in rooz tips of sunflower. Physiol Plant **53:** 354–360

Römheld V, Marschner H (1983) Mechanism of iron uptake by peanut plants. I. Fe reduction, chelate splitting, and release of phenolics. Plant Physiol **71:** 949–954

Römheld V, Marschner H (1986) Evidence for a specific uptake system for iron phytosiderophores in roots of grasses. Plant Physiol **80:** 175–180

Salama S, Stong JD, Neilands JB, Spiro TG (1978) Electronic and resonance Raman spectra of iron(III) complexes of enterobactin, catechol, and *N*-methyl-2,3-dihydroxybenzamide. Biochemistry **17:** 3781–3785

Santi S, Schmidt W (2009) Dissecting iron deficiency-induced proton extrusion in Arabidopsis roots. New Phytol **183:** 1072–1084

Schaaf G, Ludewig U, Erenoglu BE, Mori S, Kitahara T, von Wirén N (2004) ZmYS1 functions as a proton-coupled symporter for phytosiderophore- and nicotianamine-chelated metals. J Biol Chem **279:** 9091–9096

Susín S, Abián J, Sánchez-Baeza F, Peleato ML, Abadía A, Gelpí E, Abadía J (1993) Riboflavin 3′- and 5′-sulfate, two novel flavins accumulating in the roots of iron-deficient sugar beet (*Beta vulgaris*). J Biol Chem **268:** 20958–20965

Takagi S, Nomoto K, Takemoto T (1984) Physiological aspect of mugineic acid, a possible phytosiderophore of graminaceous plants. J Plant Nutr **7:** 469–477

Varotto C, Maiwald D, Pesaresi P, Jahns P, Salamini F, Leister D (2002) The metal ion transporter IRT1 is necessary for iron homeostasis and efficient photosynthesis in *Arabidopsis thaliana*. Plant J **31:** 589–599

Vert G, Grotz N, Dédaldéchamp F, Gaymard F, Guerinot ML, Briat JF, Curie C (2002) IRT1, an *Arabidopsis* transporter essential for iron uptake from the soil and for plant growth. Plant Cell **14:** 1223–1233

Welkie GW (2000) Taxonomic distribution of dicotyledonous species capable of root excretion of riboflavin under iron deficiency. J Plant Nutr **23:** 1819–1831

Yang TJW, Lin WD, Schmidt W (2010) Transcriptional profiling of the Arabidopsis iron deficiency response reveals conserved transition metal homeostasis networks. Plant Physiol **152:** 2130–2141

Yonekura-Sakakibara K, Tohge T, Matsuda F, Nakabayashi R, Takayama H, Niida R, Watanabe-Takahashi A, Inoue E, Saito K (2008) Comprehensive flavonol profiling and transcriptome coexpression analysis leading to decoding gene-metabolite correlations in *Arabidopsis*. Plant Cell **20:** 2160–2176

Yuan YX, Wu HL, Wang N, Li J, Zhao WN, Du J, Wang DW, Ling HQ (2008) FIT interacts with AtbHLH38 and AtbHLH39 in regulating iron uptake gene expression for iron homeostasis in Arabidopsis. Cell Res **18:** 385–397